DIVISION S-6—SOIL & WATER MANAGEMENT & CONSERVATION

Mapping Soil Salinity Using Calibrated Electromagnetic Measurements

S. M. Lesch,* J. D. Rhoades, L. J. Lund, and D. L Corwin

ABSTRACT

A statistical modeling approach is presented that predicts spatial soil salinity patterns from aboveground electromagnetic induction (EM) readings. In this approach, EM readings are obtained from a field sampled on a uniform (centric systematic) grid. A small number of these sample sites are chosen for soil sampling, based on the observed EM field pattern. The salinity levels for these soil samples are determined and then the remaining nonsampled salinity values are predicted from the corresponding EM readings through a multiple linear regression equation. Experimental results suggest that this approach will work well in fields having low to moderate levels of soil textural variability. For example, 95% of the spatial variability in soil salinity within typical 16.2-ha (40-acre) cotton (*Gossypium hirsutum* L.) fields could be accounted for with only 36 soil samples, as opposed to the 200 to 300 soil samples typically required if no EM readings were available. This approach makes EM readings a more practical and cost-effective tool by substantially reducing the number of soil samples needed for accurate mapping of spatial salinity patterns at the field scale.

ACCURATE SOIL SALINITY ASSESSMENT is necessary for agriculture management. Excessive soil salinity affects crop production and may cause crop loss and, eventually, land degradation. Cost-effective appraisal techniques designed to assess and monitor the salinity levels can help minimize such losses.

Field-scale soil salinity conditions can be characterized using EC_a measurements. Soil EC_a is influenced by chemical and physical properties of the soil liquid and solid phases. Soil salinity, as represented by EC_e, can be determined from field EC_a measurements (Rhoades et al., 1989b). On farmland, practical measurements of EC_a can be made with either in situ or remote devices. Three kinds of portable sensors are available: (i) four-electrode sensors, including either surface-array or insertion probes; (ii) EM induction sensors, and (iii) time domain reflectometric sensors (Rhoades and Oster, 1986; Rhoades and Miyamoto, 1990; Rhoades, 1990).

The surface-array, four-electrode, or EM techniques all give depth-weighted EC_a measurements. The weighting functions vary with the configuration of the electrodes or electromagnetic coils, frequency of electrical current used in the measurement, distribution of EC_a within the various depths of the soil profile, and other factors. All of these factors must be compensated for when interpreting soil salinity with these devices. Two approaches have been used to determine salinity by depth in the soil from EM measurements. Rhoades et al. (1989a) developed a salinity prediction model to estimate EC_e using either EM or four-electrode measurements, provided that soil water and clay content were known. Empirical equations that predict soil EC_e from EM measurements have also been developed for specific soil and water-content situations (Rhoades and Corwin, 1981; Corwin and Rhoades, 1982; Williams and Baker, 1982; Williams and Hoey, 1987; Slavich and Petterson, 1990; McKenzie et al., 1989).

For some purposes, establishing a direct EC_e = f(EM) prediction equation is advantageous, such as in a single field under uniform management where water content, bulk density, and other soil properties are reasonably homogeneous. Under such conditions, it is possible to establish an accurate EC_e–EM relationship using a limited number of soil samples. Geostatistical procedures have traditionally been used for salinity mapping when soil samples are available (Webster, 1989). However, such procedures generally require intensive sampling to obtain accurate variogram estimates. We have developed a more practical, cost-effective predictive technique—field-specific models that use limited EC_e ground-truth data and extensive EM measurements for spatial salinity predicion and mapping.

METHODS

Each field was surveyed (on a 25 by 25 m grid) using an EM-38 meter (Geonics Limited, Mississauga, ON)[1] on established spatial location coordinates. Based on the observed EM pattern, a limited number of sites were selected (as described below) for soil sampling. The EC_es of these samples were measured as described by Rhoades et al. (1989b). These data were used to estimate the parameters of the prediction model. The calibrated model was in turn used to predict the EC_e at the remaining unsampled sites from the EM measurements.

A prediction model was developed that assumed a linear relationship between the natural logarithm of the EM and EC_e values for specific soil depth increments. To increase the accuracy of salinity predictions within a specific soil depth, two EM readings were made at each survey site. One measurement was made with the coils of the EM-38 device positioned horizontally to the soil surface (EM_H) and

U.S. Salinity Lab., USDA-ARS, 4500 Glenwood Dr., Riverside, CA 92501. Contribution from the U.S. Salinity Lab. Received 4 Dec. 1990. *Corresponding author.

Published in Soil Sci. Soc. Am. J. 56:540–548 (1992).

Abbreviations: EM, electromagnetic induction; EC_a, soil electrical conductivity; EC_e, soil saturation-extract electrical conductivity; EM_H, electromagnetic induction reading taken with the coil horizontal to the soil surface; EM_V, electromagnetic induction reading taken with the soil vertical to the soil surface; MSE, mean square error.

[1]The citation of particular products or companies is for the convenience of the reader and does not imply any particular endorsement or preferential treatment by the USDA or its agents.

a second measurement with the device positioned vertically (EM_V). Both readings were incorporated into a depth-specific, multiple linear regression model:

$$\ln(EC_{z1,z2}) = B_0 + B_1[\ln(EM_H)] + B_2[\ln(EM_H) - \ln(EM_V)], \quad [1]$$

where $EC_{z1,z2}$ represents EC_e for the depth increment $z1$ to $z2$, and B_0, B_1, and B_2 are empirical regression coefficients. The difference $[\ln(EM_H) - \ln(EM_V)]$ was used in the third term, rather than $\ln(EM_V)$ to eliminate collinearity between the EM_H and EM_V readings and to reduce the variance estimates associated with the B_2 parameter. Prior to this study, EM_V had been used in equations analogous to Eq. [1] to determine EC_a and EC_e from EM measurements (Corwin and Rhoades, 1990; Rhoades et al., 1989a).

The microelevation and spatial coordinates of each site were also collected during the surveys. Incorporation of these additional variables into Eq. [1] gives:

$$\ln(EC_{z1,z2}) = B_0 + B_1[\ln(EM_H)] + B_2[\Delta EM] + B_3(r), \quad [2.1]$$

$$\text{or } \ln(EC_{z1,z2}) = B_0 + B_1[\ln(EM_H)] + B_2[\Delta EM] + B_3(x) + B_4(y), \quad [2.2]$$

where ΔEM equals $[\ln(EM_H) - \ln(EM_V)]$, r is the relative elevation, and x and y are the centered and scaled spatial coordinates. Equations [2.1] and [2.2] represent the basic models used to predict soil profile EC_e values from EM measurements for a field.

Selection of the soil sample sites was based on the concepts of response surface design theory (Box and Draper, 1987). Equation [2.1] was used as the prediction model, implying that sample sites were to be chosen based on their observed $\ln(EM_H)$, ΔEM, and microelevation readings. Sites were selected for soil sampling by first obtaining the $\ln(EM_H)$, ΔEM, and microelevation measurements across the entire field. (The initial surveys were carried out using a centric systematic sampling pattern, and encompassed 145 to 206 sites per field.) The data were separated into subsets according to their scaled EM values, defined as:

$$\text{scaled } \ln(EM_H) = [(\ln(EM_H) - \ln(EM_{H,min})]/\ln(EM_{H,max}), \quad [3]$$

where $\ln(EM_{H,min})$ and $\ln(EM_{H,max})$ represent the observed minimum and maximum $\ln(EM_H)$ readings, respectively. For each field, the scaled data were separated into nine subsets with scaled $\ln(EM_H)$ limits of (0–15%), (15–25%), (25–35%),..., (75–85%), and (85–100%). Next, within each subset, four sites were chosen that had observed ΔEM and elevation readings that most nearly mimicked an orthogonal 2^2 pattern. Overall, this design selected 36 sites for soil sampling within each EM-surveyed field.

The sampling approach is illustrated in Fig. 1. The left-hand plot shows the 206 original $\ln(EM_H)$ and ΔEM readings for Field S2A; the sixth scaled subset is identified by the overlaid rectangle. The right-hand plot shows the corresponding ΔEM and microelevation readings for the sites contained within the sixth subset. The corners of the overlaid box inside the right-hand plot identify where the four ideal ΔEM and elevation readings would have needed to occur to generate a perfectly orthogonal 2^2 design, assuming that these points were to be chosen to correspond to the 10 and 90% scaled limits of the observed data. The four points shown as diamonds represent the sites chosen for sampling and EC_e determination because they were closest to the corners of the box, and therefore represented the most nearly orthogonal design. Choosing sites in this manner within each subset ensured that the coefficients in Eq. [2.1] would be accurately estimated. Furthermore, this guaranteed that the calibrated model was not forced to extrapolate predictions much beyond the range of the sampled data.

Within each field, 36 soil samples were collected at the selected locations. The calculations involved in the selection process were carried out with a lap-top personal computer. The sites were relocated for sampling with the aid of coded stakes left at the time the EM measurements were made.

Once the EC_e values were determined on the soil samples, the parameters in Eq. [2.1] were estimated using SAS Institute (1985, p. 433–506 [GLM] and p. 655–709 [REG]). The predicted data was used to create spatial EC_e maps in natural-logarithm units. The following equation was used to convert $\ln(EC_e)$ to EC_e values:

$$EC_e = \exp[\ln(EC_e) + 0.5(s^2)], \quad [4]$$

where s^2 represents the estimated MSE term obtained during the estimation of Eq. [2.1]. This formula is simply the method of moments estimate for the mean of a log-normally distributed random variable, given the mean and variance of this variable under the logarithmic transform.

Study Area and Data Collection

Soil salinity data were collected in eight furrow-irrigated cotton fields located near Stratford, Kings County, California. Soil taxonomic descriptions are shown in Table 1 for each field. Management practices, soil properties, surface conditions, and spatial salinity patterns differed among fields. Field measurements were made in May and August of 1989 and in June 1990. Within each field, EM measurements sites were established on a centric grid with a 25-m lag spacing. The exact spatial coordinates and relative elevations of each site were measured with a Zeiss (Carl Zeiss, Oberkochen, Germany) DME theodolite system. Soil samples were collected from the 0- to 30-cm depth (and some from 30–60 cm) with a Lord (Lord Co., Santa Barbara, CA) soil-core sampler.

Table 2 presents general sampling information for the eight fields. Individual samples from specific depths were usually mixed into composite samples. Two sample extraction and compositing methods were used in 1989. In Fields S2A, S2B, and S7C, four 0- to 30-cm cores were extracted (two each from the bed and furrow) and mixed. The bed cores were taken 1 m apart beneath the EM-38 meter position. The other two samples were taken from the furrows on each side of the bed. In Fields S2C, S3C, S9A, and S8C, three cores from each site were taken and mixed into a single, composite sample. These samples were collected from one side of the bed with the Lord tube inserted at a 60° angle up from the base of the bed. The spacing between samples was 0.5 m.

In 1990, three samples were taken at each site from only either the bed or furrow, and individual cores were kept separate. Samples were taken 0.5 m apart from beneath the EM-38 measurement.

Within every field, EM_H and EM_V measurements were made at each site. These readings were taken 10 cm above the soil surface of either the furrow or the bed in both the horizontal and vertical dipole configurations. The axis of the Em-38 device was always aligned with the furrow (or bed). Soil EC_e on all the samples were measured with the paste conductance method of Rhoades et al. (1989b).

RESULTS AND DISCUSSION

An example of untransformed and logarithmically transformed EM_H vs. EC_e (0–30-cm) data (obtained for Field S2A in 1989) are shown in Fig. 2. The un-

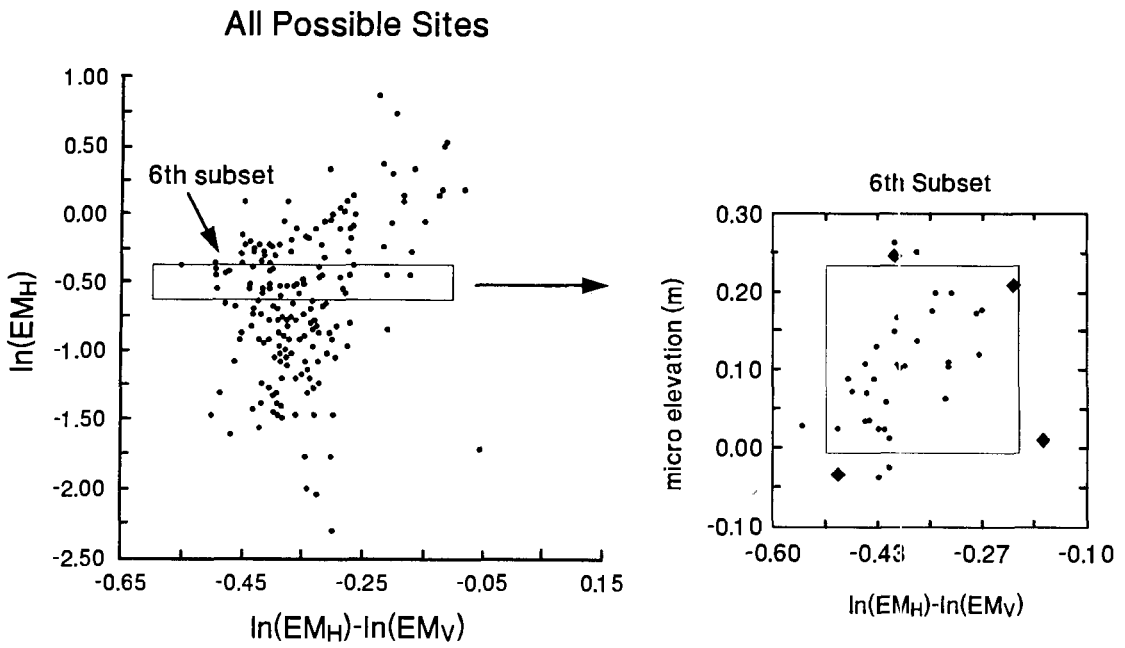

Fig. 1. Conceptual illustration of the sample site selection process using a response surface design. Points shown as diamonds represent points selected for sampling and soil saturation-extract electrical conductivity determination.

transformed relationship is nonlinear and the apparent variability increases as EM_H and EC_e increase. The relationship after the logarithmic transformation is essentially linear and the variability appears more uniform. Therefore, the linear models were calibrated with the transformed data.

Plots of $\ln(EM_V)$ vs. $\ln(EM_H)$ and $[\ln(EM_H) - \ln(EM_V)]$ vs. $\ln(EM_H)$ obtained for Field S2A (Fig. 3) show the high correlation between $\ln(EM_H)$ and $\ln(EM_V)$, but not between $\ln(EM_H)$ and ΔEM. This is one reason why the ΔEM difference, rather than $\ln(EM_V)$, was used in the regression model as the second variable. Such plots can also identify errors or unusual sites before site selection begins. For example, Site A appears clearly unusual in the second plot (Fig. 3b), but not the first.

Parameter estimates for Eq. [2.1] obtained from both the full data sets and the 36 sites selected by the sampling design are shown in Table 3. The estimated coefficients from only 36 sites were close to those from the entire data within each field. In no case did these estimates vary more than two standard deviations.

Correlation coefficients of the two sets of predicted $\ln(EC_e)$ (Table 4) generally exceeded 0.99, confirming that there was little loss in prediction accuracy when coefficients based on only 36 samples were used. Table 4 also shows the variance (MSE) estimates for the prediction equations from both data sets. Variance estimates based on 36 samples were usually within 20 to 30% of the MSE estimates using all the data.

In Table 5, the measured and predicted EC_e per se are compared in terms of mean and percentile statistics. The back-transformed EC_e predictions were good, though there were exceptions, for example, the 30- to 60-cm EC_e of Field S3C. Predictions were also typically less accurate for the fifth and 95th percentiles. However, estimates of mean predicted EC_e and 10th through 90th percentiles were reliable, implying that most of the observed salinity range within each field was well estimated.

Table 1. Soil taxonomic classifications for the eight selected fields.

Field	Taxonomic class
S2A, S9A	Coarse-loamy, mixed, thermic Typic Salorthid
S2B, S2C, S32	Coarse-loamy, mixed (calcareous), thermic Aeric Haplaquent
S7C	Coarse-loamy, mixed, thermic Fluvaquentic Haploxeroll
S3C, S8C	Fine-loamy, mixed (calcareous), thermic Fluvaquentic Haplaquoll

Tables 3, 4, and 5 confirm that the parameters in Eq. [2.1] could be accurately estimated from a minimum number (36) of carefully chosen sample sites. However, prediction equations such as Eq. [2.1] are of little use unless they can successfully estimate the true salinity pattern across the survey area. An example of the spatial agreement between predicted $\ln(EC_e)$, based on 36 samples, and observed $\ln(EC_e)$ is shown in Fig. 4 for Field S2A. Although the predicted salinity pattern corresponds reasonably well with the actual pattern, some discrepancies exist. The amount of disagreement between the predicted and observed patterns shown in Fig. 4 was representative of that found for most of the other fields surveyed in 1989.

A possible explanation for the above-mentioned disagreement could have been the failure of the regression approach to account for spatial correlation between neighboring sample sites. It could also have been due to high variability across the field in other soil properties (e.g., texture, water content, or temperature) that the model assumed to be homogeneous. Since soil properties should themselves be spatially dependent, this type of error can be deduced by examining the residuals (from Eq. [2.1]) for spatial au-

Table 2. General soil sampling information for the eight selected fields.

Field	Sampling date	Sample sites	Soil depth	Field size	Saturation	
					Mean	90% range†
	mo/yr	no.	m	ha	%	
S2A	5/89	206	0–0.3	15.0	35.9	27.6–43.5
S2B	5/89	193	0–0.3	13.9	35.7	29.0–43.2
S7C	5/89	188	0–0.3	14.2	43.5	32.7–52.4
S2C	7/89	195	0–0.3	13.7	32.8	26.7–38.1
	7/89	195	0.3–0.6	13.7	33.3	25.2–43.0
S3C	7/89	145	0–0.3	12.5	34.5	30.4–40.3
	7/89	145	0.3–0.6	12.5	36.1	30.3–43.3
S9A	7/89	167	0–0.3	16.1	37.1	31.0–47.2
	7/89	167	0.3–0.6	16.1	42.6	30.3–58.7
S8C	8/89	191	0–0.3	13.5	39.6	31.9–49.1
	8/89	191	0.3–0.6	13.5	42.9	31.1–59.2
S2A‡	6/90	36§	0–0.3	11.7	37.6	29.2–45.3
S32	6/90	36§	0–0.3	12.0	35.7	28.3–42.2

† The 90% range for the water content represents data falling between the fifth and 95th percentiles.
‡ 25% less total area was sampled within this field during the June 1990 survey.
§ Three soil samples per depth were taken within these fields.

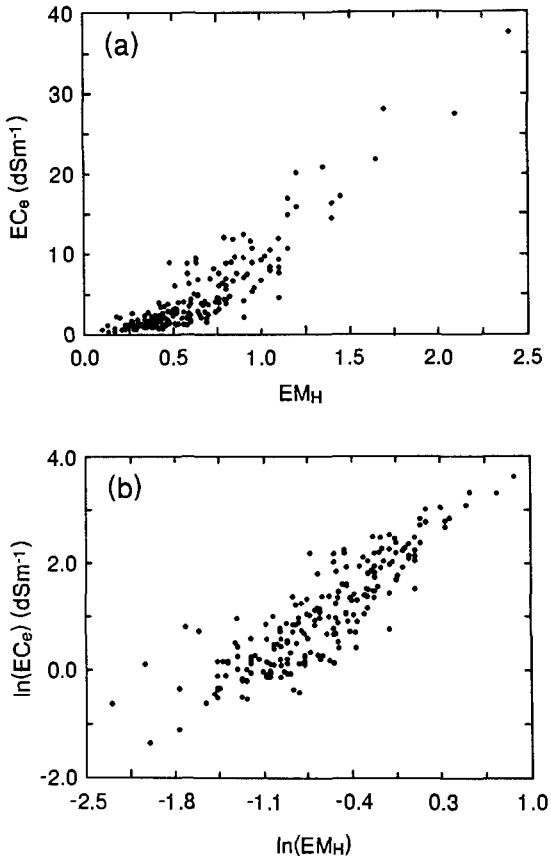

Fig. 2. Comparison of (a) electromagnetic induction readings taken with the coil horizontal to the soil surface (EM_H) vs. soil saturation-extract electrical conductivity (EC_e) data (0–30 cm) and (b) natural-log-transformed EM_H vs. natural-log-transformed EC_e (0–30 cm) data for Field S2A.

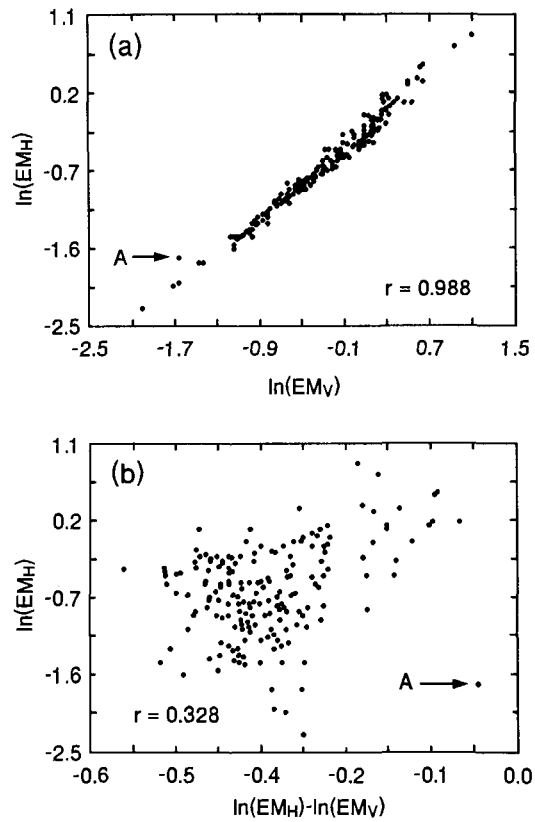

Fig. 3. Correlation plots indicating (a) the high degree of collinearity between the natural-log-transformed data for electromagnetic reduction readings taken with the coils horizontal to the soil surface (EM_H) and those taken with the coils held vertically (EM_V), and (b) the elimination of this collinearity by using the difference between these readings as the second variable.

tocorrelation. Variograms of the observed $\ln(EC_e)$ (Fig. 5) for Field S2A show distinct spatial covariance in the $\ln(EC_e)$ data, with the variance increasing as the lag distance between sample sites increased. However, this spatial covariance is missing in the residuals. Variograms of the residuals within the remaining 1989 fields also revealed little spatial covariance. Based on these results, we concluded that the primary source of prediction error was not due to variability of the soil physical properties.

Another possible explanation for the prediction error, apparent in Fig. 4, is that the measured values of EC_e are not representative of the larger soil volume included in the EM_H and EM_V measurements. The three-dimensional salinity pattern can be quite variable in the furrow-bed environment of irrigated soils,

Table 3. Calculated parameter coefficients and their associated standard error (in parentheses) for Eq. [2.1].

Field	Soil Depth	Sample sites	Calculated parameter coefficients B_0	B_1	B_2	B_3
	cm	no.				
S2A	0–30	206	2.258 (0.18)	1.488 (0.06)	1.462 (0.43)	1.978 (0.48)
	0–30	36	2.231 (0.33)	1.372 (0.12)	1.601 (0.79)	2.133 (0.99)
S2B	0–30	193	2.403 (0.11)	1.194 (0.07)	1.674 (0.20)	1.348 (0.80)
	0–30	36	2.105 (0.22)	1.124 (0.15)	1.314 (0.41)	2.940 (1.5)
S7C	0–30	188	2.541 (0.07)	1.105 (0.04)	1.194 (0.20)	0.025 (0.15)
	0–30	36	2.460 (0.12)	1.124 (0.08)	0.815 (0.36)	0.039 (0.33)
S2C	0–30	195	1.697 (0.33)	1.278 (0.08)	2.431 (0.49)	0.602 (0.55)
	0–30	36	1.296 (0.51)	1.425 (0.13)	0.956 (0.76)	0.868 (0.84)
	30–60	195	1.690 (0.32)	1.485 (0.08)	1.962 (0.47)	1.796 (0.54)
	30–60	36	1.125 (0.56)	1.529 (0.14)	0.699 (0.84)	2.334 (0.92)
S3C	0–30	145	4.497 (0.51)	1.667 (0.15)	3.274 (0.80)	−3.413 (0.74)
	0–30	36	5.067 (0.85)	1.293 (0.24)	4.441 (1.3)	−3.885 (1.1)
	30–60	145	3.658 (0.49)	2.546 (0.15)	1.837 (0.76)	−0.680 (0.71)
	30–60	36	4.947 (0.79)	2.290 (0.22)	3.341 (1.2)	−2.418 (1.0)
S9A	0–30	167	0.443 (0.27)	1.185 (0.10)	2.260 (0.48)	3.562 (0.45)
	0–30	36	0.674 (0.50)	0.959 (0.20)	2.939 (0.88)	3.334 (0.88)
	30–60	167	0.980 (0.28)	1.887 (0.10)	0.837 (0.50)	3.063 (0.46)
	30–60	36	1.632 (0.63)	1.875 (0.25)	2.262 (1.1)	1.891 (1.1)
S8C	0–30	191	1.035 (0.20)	1.156 (0.06)	1.353 (0.31)	1.482 (0.34)
	0–30	36	1.062 (0.39)	1.275 (0.14)	1.394 (0.59)	1.440 (0.74)
	30–60	191	1.134 (0.19)	1.300 (0.06)	−0.251 (0.29)	1.904 (0.31)
	30–60	36	1.076 (0.33)	1.346 (0.12)	−0.138 (0.50)	2.082 (0.64)

due to the leaching of salts beneath the furrow and the accumulation of salts in the bed caused by mass flow and evaporation. To better visualize the error components inherent in the sampling design, consider the variability sources contributing to the total MSE estimate. The MSE can be separated into four general components:

$$\text{MSE} = S_1 + S_2 + S_3 + S_4. \quad [5]$$

In Eq. [5], S_1, S_2, S_3, and S_4 represent the error caused by differences in the soil physical properties, soil water content, deep (1–2 m) profile salinity sensed by the EM-38, and salinity variation in the bed–furrow microenvironment, respectively. The first three error terms represent lack-of-fit errors, because they reduce the salinity prediction accuracy. However, uncertainty related to S_4 does not cause reductions in the model's predictive capability. The soil volume sensed by the EM measurement is much larger than that sampled for EC_e appraisal and EC_e can be quite variable within the bed–furrow system. Thus, it is reasonable to assume that the salinity-prediction model contains two general types of errors: the within-site error of high salinity variability in the microenvironment of the bed–furrow system, and the between-site error caused by soil property variations other than salinity. The between-site variance is the appropriate error term for evaluating the prediction equation.

The 1990 field studies were conducted to determine how much of the total prediction error could be attributed to the within-site error component. In these studies, three soil samples from either the bed (Field S32) or the furrow (Field S2A) were collected at each of the 36 sites and separately analyzed for EC_e. These separate values of EC_e were used to estimate the within-site error of the EC_e ground truth. The method used to partition the residual sum of squares into within-site and between-site error components was equivalent to the standard approach used to estimate "pure" and lack-of-fit error components in a regression equation with repeated experimental runs (Myers, 1986).

Table 4. Summary statistics for Eq. [2.1], using all the soil samples from each field and the restricted (36-site) data sets only.

Field	Soil depth	All sample sites† MSE	All sample sites† R^2	36 selected sites only MSE	36 selected sites only R^2	Correlation‡ (between predictions)
	cm					
S2A	0–30	0.178	0.813	0.232	0.841	0.9992
S2B	0–30	0.139	0.712	0.191	0.760	0.9937
S7C	0–30	0.049	0.890	0.069	0.903	0.9989
S2C	0–30	0.346	0.708	0.284	0.838	0.9892
	30–60	0.325	0.773	0.340	0.847	0.9946
S3C	0–30	0.698	0.663	0.656	0.753	0.9912
	30–60	0.635	0.768	0.560	0.870	0.9909
S9A	0–30	0.273	0.626	0.357	0.708	0.9864
	30–60	0.290	0.710	0.559	0.716	0.9864
S8C	0–30	0.183	0.704	0.254	0.766	0.9995
	30–60	0.155	0.744	0.186	0.807	0.9996

† Information on the exact number of sample sites is given in Table 2.
‡ Correlation between predicted log saturation-extract electrical conductivity (EC_e) values using both sets of parameter estimates (for Eq. [2.1]) shown in Table 2.

The ability to adapt the prediction equation to specific field characteristics was exploited during the model-building stage. Equations [2.1] and [2.2] were each fit using microelevation and spatial-coordinate data acquired during the initial survey. The model with the best prediction accuracy (e.g., smallest MSE) was then validated using the residual diagnostics of Weisberg (1985) and Atkinson (1985).

Summary statistics for two prediction models fit to the 1990 field data are given in Table 6. The first model is a modification of Eq. [2.2] and the second

Table 5. Observed and predicted values of saturation-extract electrical conductivity (EC_e) in terms of mean and percentile statistics.

Field	Soil depth	Data set	Mean	SE§	Percentiles						
					5th	10th	25th	50th	75th	90th	95th
	cm		dS m^{-1}								
S2A	0–30	obs†	4.496	0.367	0.70	0.89	1.22	2.47	6.07	9.73	14.9
		prd‡	4.637	0.373	0.98	1.13	1.85	2.78	5.60	9.44	15.5
S2B	0–30	obs	6.627	0.336	1.29	2.03	3.64	6.04	8.58	11.3	12.6
		prd	6.635	0.269	1.31	2.93	3.98	5.99	7.97	11.6	13.8
S7C	0–30	obs	19.57	0.857	5.63	7.28	11.7	16.3	25.4	37.4	42.5
		prd	20.20	0.802	5.44	6.39	12.5	18.3	25.8	37.3	44.7
S2C	0–30	obs	2.228	0.236	0.34	0.39	0.54	0.68	1.99	8.00	9.40
		prd	2.109	0.162	0.35	0.45	0.72	1.22	2.67	5.55	7.14
S2C	30–60	obs	3.446	0.302	0.31	0.44	0.74	1.34	4.72	10.5	12.9
		prd	3.689	0.327	0.45	0.65	1.10	1.90	4.66	9.68	12.3
S3C	0–30	obs	3.112	0.331	0.17	0.21	0.40	1.59	4.16	8.07	12.4
		prd	3.693	0.365	0.41	0.65	0.95	2.04	4.91	8.89	10.0
S3C	30–60	obs	5.327	0.441	0.06	0.13	0.82	4.06	7.90	11.4	16.4
		prd	7.765	1.123	0.35	0.51	1.08	3.11	7.83	17.9	27.1
S9A	0–30	obs	4.315	0.251	0.84	0.93	1.47	3.59	6.33	8.96	10.8
		prd	4.680	0.245	1.32	1.64	2.42	3.85	5.93	8.88	10.3
S9A	30–60	obs	7.406	0.392	0.71	1.10	3.66	6.70	10.3	14.5	17.6
		prd	8.015	0.537	1.31	1.80	3.31	5.82	10.7	15.7	22.0
S8C	0–30	obs	6.334	0.376	1.24	1.61	2.74	4.65	8.28	12.1	16.7
		prd	7.177	0.379	1.68	2.17	3.76	5.95	8.21	13.9	18.4
S8C	30–60	obs	14.27	0.561	1.54	4.46	8.97	14.1	18.0	24.0	28.7
		prd	15.41	0.744	3.74	5.09	8.97	13.3	18.6	26.8	37.7

† Observed EC_e, all sample sites included.
‡ Predicted EC_e, from Eq. [2.1] (calibrated with 36-sample sites only).
§ Standard error of the mean.

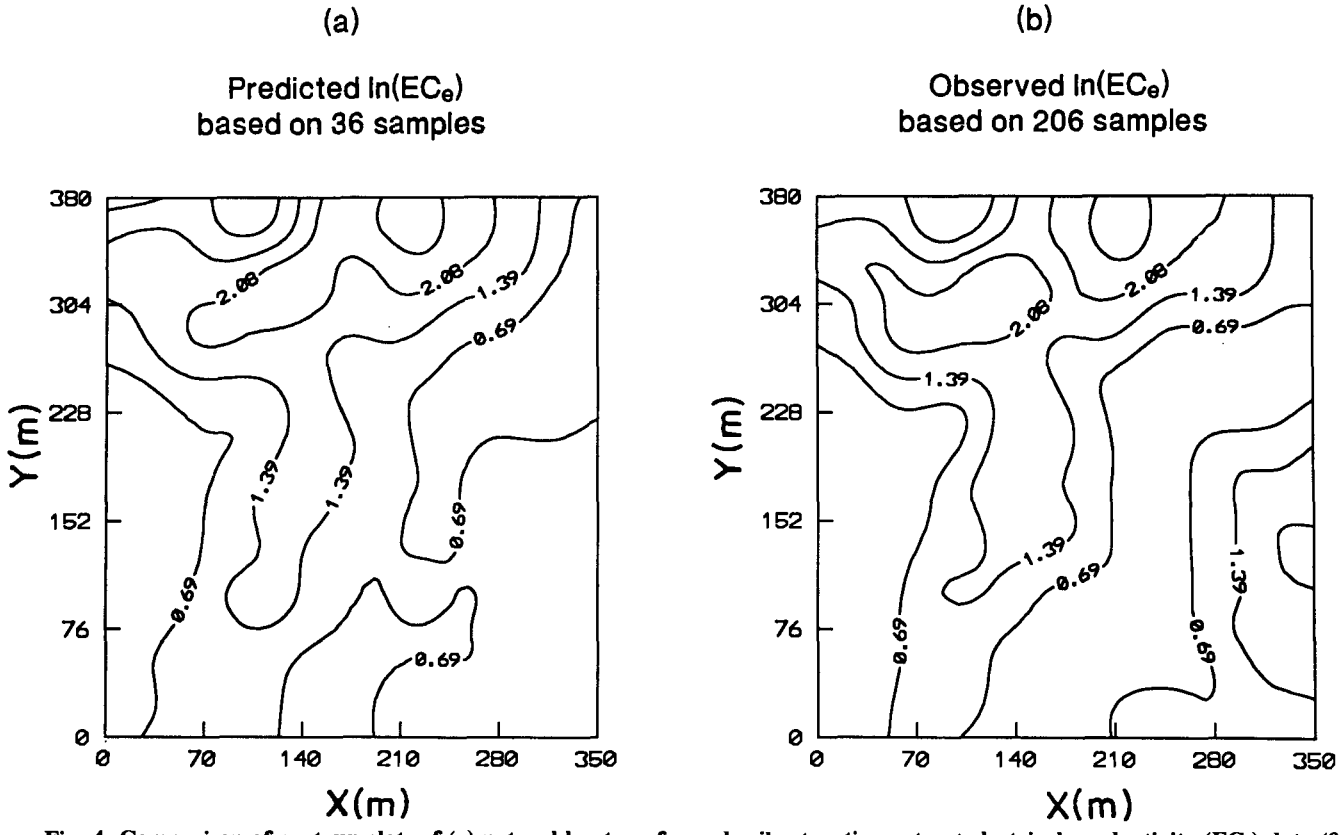

Fig. 4. Comparison of contour plots of (a) natural-log-transformed soil saturation-extract electrical conductivity (EC_e) data (0–30 cm) derived from the prediction equation based on 36 samples and (b) observed natural-log-transformed EC_e (0–30 cm) values for Field S2A.

Table 6. Analysis of variance for Fields S2A and S32, using natural-log-transformed soil saturation-extract electrical conductivity (EC_e) data acquired in 1990.

Source	df	Sum of squares	Mean square	*F*-test	*P* > *F*	R^2
Field S2A						
Model	5	132.4214	26.4843	190.02	0.0001	0.903
Error	102	14.2167	0.1394			
Between-site	30	8.0397	0.2680			
Within-site	72	6.1773	0.0858			
Total	107	146.6381				
Within-site variance estimate = 0.0858						
Between-site variance estimate (0.2680 − 0.0858)/3 = 0.0607						
Variability table						
Model 90.30%						
Within-site error 5.68%						
(Total explained variability) 95.98%						
Between-site error 4.02%						
Field S32						
Model	4	138.3806	34.5952	248.27	0.0001	0.906
Error	103	14.3526	0.1393			
Between-site	31	9.0557	0.2921			
Within-site	72	5.2969	0.0736			
Total	107	152.7332				
Within-site variance estimate = 0.0736						
Between-site variance estimate (0.2921 − 0.0736)/3 = 0.0728						
Viability Table						
Model 90.60%						
Within-site error 4.73%						
(Total explained variability) 95.33%						
Between-site error 4.67%						

is adapted from Eq. [2.1]. For Field S2A, the residual analysis revealed a strong linear trend when plotted against both the x and y coordinates. Thus, a first-order, linear trend surface (including an interaction term) was incorporated into the model to give

$$\ln(EC_e) = B_0 + B_1[\ln(EM_H)] + B_2[\Delta EM] + B_3(x) + B_4(y) + B_5(xy), \quad [6]$$

where x and y represent the centered and scaled coordinates of the sample sites.

For Field S32, the residual analysis revealed a systematic, nonlinear relationship between the residuals and $\ln(EM_H)$. An interaction term was incorporated into the model to alleviate this problem, yielding

$$\ln(EC_e) = B_0 + B_1[\ln(EM_H)] + B_2[\Delta EM] + B_3[\ln(EM_H)\,\Delta EM] + B_4(r). \quad [7]$$

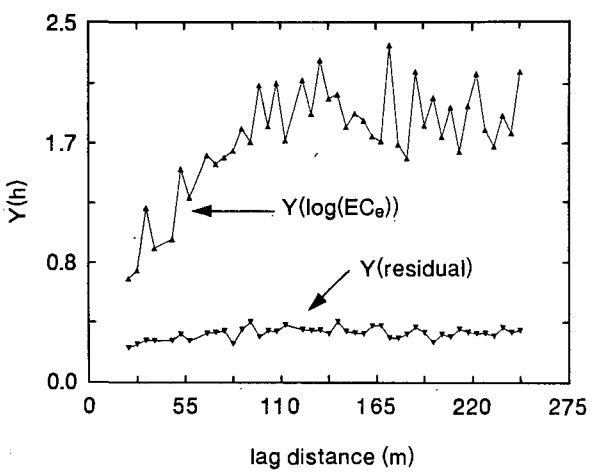

Fig. 5. Variograms of the observed natural-log-transformed soil saturation-extract electrical conductivity (EC_e) and residuals for Field S2A, 1989 soil sample data.

Both models permitted accurate prediction of EC_e, accounting for 90 to 91% of the observed salinity variability. The within-site sampling error accounted for an additional 4 to 5% of the variability. Taken together, about 95% of the total observed variability was explainable by the prediction equations and micro salinity variations.

Because the number of samples analyzed for EC_e in the study summarized in Table 6 was increased three-fold (3 × 36), a means of reducing this number was sought. The original 36 sites were systematically partitioned into two sets of 18 sites and only the two outside soil cores were used as EC_e calibration data. In this way, the total number of calibration samples in each data set was reduced from 108 to 36, as in 1989. Equivalent estimates of model coefficients and explained variability were obtained using either of the 18-site data sets (Table 7). Since the two sets were mutually exclusive (no sample in the first set was included in the second, or vice versa), it was possible to formally test the equivalence of these prediction models. This was done using a general *F*-test, by nesting the prediction models together and testing for equivalent parameter estimates (Weisberg, 1985). In both fields, the two prediction models fitted to each 18-site data set were statistically equivalent.

Plots of predicted vs. observed soil salinity for Field S2A are shown in Fig. 6 in log-EC_e units. The calibration data correspond to the 18 sites within the first data set. They were the data used in developing the coefficients for Eq. [6], shown in Table 6, Column

Table 7. Calculated parameter coefficients and their associated standard errors in parentheses for Eq. [6] and [7] found using both the full data sets (36 sites, three samples per site) and two mutually exclusive subsets (18 sites, two samples per site).

Field	Parameter	Estimates		
			Partitioned subsets	
		Full data set	A	B
S2A	B_0	2.019 (0.06)	2.116 (0.15)	1.996 (0.10)
	B_1	1.221 (0.05)	1.217 (0.11)	1.245 (0.10)
	B_2	1.874 (0.35)	2.357 (0.84)	1.612 (0.56)
	B_3	−0.268 (0.05)	−0.209 (0.12)	−0.319 (0.09)
	B_4	0.353 (0.03)	0.298 (0.07)	0.399 (0.06)
	B_5	0.114 (0.05)	0.158 (0.11)	0.130 (0.09)
Total explained variability		95.98	96.44	97.21
S32	B_0	2.530 (0.09)	2.627 (0.11)	2.443 (0.19)
	B_1	1.032 (0.08)	0.901 (0.10)	1.108 (0.16)
	B_2	2.041 (0.31)	1.976 (0.38)	1.942 (0.65)
	B_3	−2.102 (0.40)	−2.211 (0.52)	−1.965 (0.79)
	B_4	1.689 (0.67)	1.150 (0.92)	2.100 (1.2)
Total explained variability		95.33	95.67	97.67

A. The prediction data correspond to validation data (average EC_e) for sites within the second set; these sites were not used for estimating the parameters in Column A. This plot shows a good 1:1 correspondence between observed and predicted soil salinity using a sampling design employing 18 sites and two samples per site for calibration purposes.

CONCLUSIONS

Soil salinity was accurately mapped within individual fields under uniform management from an intensive set of EM measurements and a regression model (prediction equation) calibrated for each field with minimal soil sampling. Aboveground instrument readings (EM data, microelevation data) were used to specify sites for soil sampling. By applying the concepts of response surface design theory to the site-selection process, accurate and stable parameter estimates were acquired (i.e., a well-calibrated model) and the guesswork involved in selecting the sample site locations was simultaneously removed.

Soil property variability other than salinity present in the fields studied in 1990 did not appreciably affect the prediction-equation accuracy. However, the method is not recommended for fields with substantial soil property heterogeneity other than salinity. For heterogeneous fields, geostatistical techniques (e.g., cokriging) should be used.

The adequacy of the homogeneity assumption was determined from partitioning the MSE estimate. A large between-site error, compared with the within-site error, should be interpreted as an indication of field heterogeneity. To facilitate such an MSE partitioning, soil sampling techniques for calibration purposes were used that separated microenvironment salinity variations from field-scale variations.

The advantages of this method were the rapidity and easy of the EM measurements and the relatively small number of soil samples that needed to be analyzed. The disadvantages were that the fields had to be entered a second time for soil sampling after all the EM readings were taken, and the sample site locations had to be determined using computer calculations. Additionally, this method may produce biased

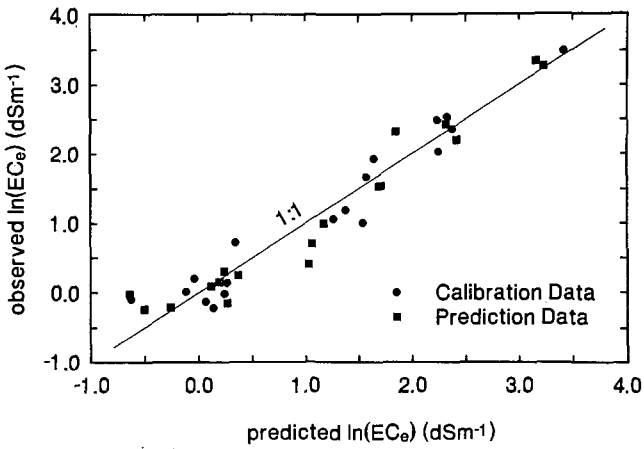

Fig. 6. Plot of the predicted vs. observed values of natural-log-transformed salinity (0–30 cm) for Field S2A, 1990 soil sample data.

EC_e estimates in fields that are very heterogeneous with respect to soil texture or water content.

REFERENCES

Atkinson, A.C. 1985. Plots, transformations and regression: An introduction to graphical methods of diagnostic regression analysis. Clarendon Press, Oxford, England.

Box, G.E.P., and N.R. Draper. 1987. Empirical model-building and response surfaces. John Wiley & Sons, New York.

Corwin, D.I., and J.D. Rhoades. 1982. An improved technique for determining soil electrical conductivity—Depth relations from aboveground electromagnetic measurements. Soil Sci. Soc. Am. J. 46:517–520.

Corwin, D.L., and J.D. Rhoades. 1990. Establishing soil electrical conductivity—Depth relations from electromagnetic induction measurements. Commun. Soil Sci. Plant Anal. 21:861–901.

McKenzie, R.C., W. Chomistek, and N.F. Clark. 1989. Conversion of electromagnetic inductance readings to saturated paste extract values in soil for different temperature, texture, and moisture conditions. Can. J. Soil Sci. 69:25–32.

Myers, R.H. 1986. Classical and modern regression with applications. Duxbury Press, Boston, MA.

Rhoades, J.D. 1990. Soil salinity: Causes and controls. p. 109–134. *In* A.S. Goudie (ed.) Techniques for desert reclamation. John Wiley & Sons, New York.

Rhoades, J.D., and D.L. Corwin. 1981. Determining soil electrical conductivity—Depth relations using an inductive electromagnetic soil conductivity meter. Soil Sci. Soc. Am. J. 42:255–260.

Rhoades, J.D., S.M. Lesch, P.J. Shouse, and W.J. Alves. 1989a.

New calibrations for determining soil electrical conductivity—Depth relations from electromagnetic measurements. Soil Sci. Soc. Am. J. 53:74–79.

Rhoades, J.D., N.A. Manteghi, P.J. Shouse, and W.J. Alves. 1989b. Soil electrical conductivity and soil salinity: New formulations and calibrations. 14 53:433–439.

Rhoades, J.D., and S. Miyamoto. 1990. Testing soils for salinity and sodicity. p. 299–336. *In* P.L. Westerman (ed.) Soil testing and plant analysis. 3rd ed. SSSA Book Ser. no. 3, SSSA, Madison, WI.

Rhoades, J.D., and J.D. Oster. 1986. Solute content. p. 985–1006. *In* A. Klute (ed.) Methods of soil analysis. Part 1. 2nd ed. Agron. Monogr. 9. ASA and SSSA, Madison, WI.

SAS Institute. 1985. SAS users guide: Statistics. Version 5 ed. SAS Inst., Cary, NC.

Slavich, P.G., and G.H. Petterson. 1990. Estimating average rootzone salinity from electromagnetic induction (EM-38) measurements. Aust. J. Soil Res. 28:453–463.

Webster, R. 1989. Recent achievements in geostatistical analysis of soil. Agrokem. Talajtan 38:519–536.

Weisberg, S. 1985. Applied linear regression. John Wiley & Sons, New York.

Williams, B.G., and G.C. Baker. 1982. An electromagnetic induction technique for reconnaissance surveys of soil salinity hazards. Aust. J. Soil Res. 20:108–118.

Williams, B.G., and D. Hoey. 1987. The use of electromagnetic induction to detect the spatial variability of the salt and clay contents of soils. Aust. J. Soil Res. 25:21–27.